

# Effects of the Wavy Surface on Free Convection-Radiation along an Inclined Plate

M. Si Abdallah and B. Zeghamati

**Abstract**—A numerical analysis used to simulate the effects of wavy surfaces and thermal radiation on natural convection heat transfer boundary layer flow over an inclined wavy plate has been investigated. A simple coordinate transformation is employed to transform the complex wavy surface into a flat plate. The boundary layer equations and the boundary conditions are discretized by the finite difference scheme and solved numerically using the Gauss-Seidel algorithm with relaxation coefficient. Effects of the wavy geometry, the inclination angle of the wavy plate and the thermal radiation on the velocity profiles, temperature profiles and the local Nusselt number are presented and discussed in detail.

**Keywords**—Free convection, wavy surface, inclined surface, thermal radiation.

## I. INTRODUCTION

NATURAL convection flow and heat transfer along a surface is present in many processes in nature and in engineering devices. Examples of free convection flows can be found in atmospheric flows, heat exchangers, solar energy collectors, drying technologies, food processing, and cooling of electronic systems.

Previous studies of natural convection heat and mass transfer have focused mainly on a flat plate or regular ducts. Adams and Fadden [1] experimentally studied the free convection with opposing body force. Yao [2] performed a numerical study of the natural convection along a wavy surface. The results show that the frequency of the local heat transfer rate is twice that of the flat surface. The amplitude of the oscillating local Nusselt number gradually decreases downstream where the natural convection boundary layer becomes thick. Ching-Yang [3] analyzed the free convection heat and mass transfer near a vertical wavy surface in a porous medium. Both the wall temperature and concentration are assumed to be constant. The results show that increasing the buoyancy ratio leads to increase both the Nusselt and Sherwood numbers. Kefeng and Wen-Qiang [4] numerically analyzed the magnitude of the buoyancy ratio on the double-diffusive convection in a vertical cylinder with radial temperature and axial solute gradients for different values of Grashof, Prandtl and Schmidt numbers. Jer-Huan et al. [5] investigated the effects of the wavy surface on natural convection heat and mass transfer. A marching finite

difference scheme is used for this analysis. The higher amplitude-wavelength ratio increases the fluctuation of velocity, temperature and concentration, while, the skin-friction coefficient, Nusselt number, and Sherwood number are smaller for amplitude- wavelength. Lin et al. [6] studied the free convection on an arbitrarily inclined plate with uniform surface heat flux. Simple correlation equations are obtained for arbitrary inclination from the horizontal to the vertical and for  $0.001 \leq Pr \leq \infty$ . Shyam et al. [7] studied the MHD free convection radiation interaction along a vertical surface embedded in Darcian porous medium in presence of Soret and Dufour's effects. It is found that the Nusselt number increases and Sherwood number decreases as the radiation parameter increases but both the Nusselt number and Sherwood number decrease as the magnetic field parameter increases. The interaction of radiation with free convection in porous media has also been studied by many researchers. Whitaker [8] studied the radiant energy transport in porous media. Chandrasekhara et al. [9] considered the composite heat transfer in the case of flow past a horizontal surface embedded in a saturated porous medium. Raptis [10], using Rosseland approximation for radiative heat flux, studied the free convection flow through porous medium. Hossain et al. [11] studied the effect of radiation on free convection from an inclined surface placed in Darcian porous media. Chamkha [12] studied solar radiation assisted free convection from a vertical plate in a porous medium with a more general Darcy-Forchheimer-Brinkman flow.

## II. ANALYSIS

A schematic diagram of semi-infinite inclined wavy plate is shown in Fig. 1. The wavy surface is described by:

$$y = \sigma^*(x) = a^* \sin(2\pi x/L)$$

M. Si Abdallah is with the Physics Department, Faculty of Sciences, University of M'Sila, Algeria (Fax: +213 35-55-44-79; (e-mail: s\_maayouf@yahoo.fr).

B. Zeghamati is with the Laboratoire de Mathématiques et Physique, Université de Perpignan Via Domitia, France (e-mail: zeghamati@univ-pepr.fr).

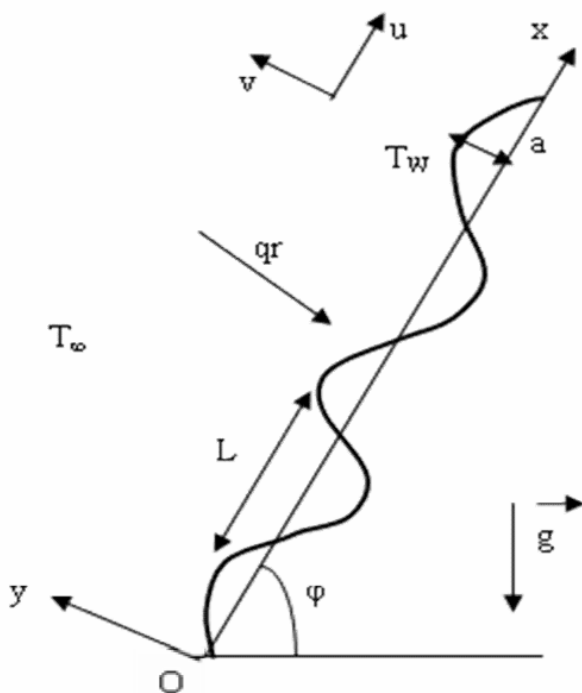


Fig. 1 Physical model and coordinate system

where  $a^*$  is the amplitude of the wavy surface and  $L$  is the characteristic wavelength. It is assumed that the surface is kept at constant temperature  $T_w$  different that the ambient one  $T_\infty$ . The wavy plate is heated and provides heat flux radiation  $q_r$  to the fluid and  $\phi$  is the inclination angle of the wavy plate from the horizontal, in this problem we consider that  $\phi$  is in the range ( $20^\circ$ – $90^\circ$ ). The origin of the Cartesian coordinates system  $(x, y)$  is placed at the leading edge of the surface. The  $u$  and  $v$  are the velocity components in the  $x$  and  $y$  direction respectively. It is assumed that the fluid is Newtonian and incompressible. All the physical properties of the fluid are assumed to be constants except for the density variation in the buoyancy term in the momentum equation. The flow is steady and laminar. Under these assumptions, the governing equations can be written in two-dimensional Cartesian coordinates  $(x, y)$  as:

Continuity equation

$$\frac{\partial u}{\partial x} + \frac{\partial v}{\partial y} = 0 \quad (1)$$

Momentum equation

$$u \frac{\partial u}{\partial x} + v \frac{\partial u}{\partial y} = -\frac{1}{\rho} \frac{\partial p}{\partial x} + \nu \left( \frac{\partial^2 u}{\partial x^2} + \frac{\partial^2 u}{\partial y^2} \right) + g\beta (T - T_\infty) \sin(\phi) \quad (2)$$

$$u \frac{\partial v}{\partial x} + v \frac{\partial v}{\partial y} = -\frac{1}{\rho} \frac{\partial p}{\partial y} + \nu \left( \frac{\partial^2 v}{\partial x^2} + \frac{\partial^2 v}{\partial y^2} \right) + g\beta (T - T_\infty) \cos(\phi) \quad (3)$$

Energy Equation

$$\rho c_p \left( u \frac{\partial T}{\partial x} + v \frac{\partial T}{\partial y} \right) = k \left( \frac{\partial^2 T}{\partial x^2} + \frac{\partial^2 T}{\partial y^2} \right) - \frac{\partial q_r}{\partial y} \quad (4)$$

The quantity  $q_r$  on the right-hand side of (4) represents the radiative heat flux in the  $y$  direction. For simplicity and comparison, the radiative heat flux term in the energy equation is analyzed by utilizing the Rosseland diffusion approximation [13] for an optically thick boundary layer as follows:

$$q_r = \frac{4\sigma_B}{3\alpha_R} \frac{\partial T^4}{\partial y} \quad \text{and} \quad \frac{\partial q_r}{\partial y} = \frac{4\sigma_B}{3\alpha_R} \frac{\partial T^3}{\partial y} \quad (5)$$

where  $\sigma_B$  is the Stefan-Boltzmann constant and  $\alpha_R$  is the mean absorption coefficient.

The appropriate boundary conditions for (1)-(4) are:

$$\begin{aligned} \text{at the wavy surface, } y = \sigma^*(x): u=0, v=0, T = T_w \\ y \rightarrow \infty: \text{ the flow is quiescent : } u=0, T = T_\infty \end{aligned}$$

In order to avoid the non-uniformity of the mesh spacing in the vicinity of the wavy surface, the physical domain is transformed into a flat surface using the following transformation:

$$x^* = \frac{x}{L}; \quad y^* = \frac{y - \sigma^*(x)}{L} Gr^{1/4} \quad (6)$$

Moreover, the following non-dimensional variables are introduced

$$\begin{aligned} u^* &= \frac{L}{\nu Gr^{1/2}} u; \quad v^* = \frac{L}{\nu Gr^{1/4}} (v - u_x) = \frac{L}{\mu^2 Gr} v \\ Gr &= \frac{g \beta (T_w - T_\infty) L^3}{\nu^2} \quad a = \frac{a^*}{L}; \quad \theta = \frac{T - T_\infty}{T_w - T_\infty} \\ &= \frac{T - T_\infty}{T_w - T_\infty} = \frac{p}{k} = \frac{1}{\infty} = \frac{T_\infty}{T_w - T_\infty} \end{aligned} \quad (7)$$

The dimensionless form of the (1)-(4) in the new coordinate system  $(x^*, y^*)$ , after ignoring terms of small orders in  $Gr$  is:

$$\frac{\partial u^*}{\partial x^*} + \frac{\partial v^*}{\partial y^*} = 0 \quad (8)$$

$$u^* \frac{\partial u^*}{\partial x^*} + v^* \frac{\partial u^*}{\partial y^*} = -\frac{\partial p^*}{\partial x^*} + \sigma_x \frac{\partial P^*}{\partial y^*} Gr^{1/4} + \quad (9)$$

$$\begin{aligned} (1 + \sigma_x^2) \frac{\partial^2 u^*}{\partial y^{*2}} + \theta \sin(\phi) \\ \sigma_{xx} u^{*2} = -\frac{\partial p^*}{\partial y^*} Gr^{1/4} + \theta \cos(\phi) \end{aligned} \quad (10)$$

$$u^* \frac{\partial \theta}{\partial x^*} + v^* \frac{\partial \theta}{\partial y^*} = \frac{1 + \sigma_x^2}{Pr} \frac{\partial^2 \theta}{\partial y^{*2}} + \frac{16 \sigma_B}{3 \alpha_R} \frac{\theta^3 \Delta T^3}{\mu Cp} \frac{\partial^2 \theta}{\partial y^{*2}} \quad (11)$$

For the current problem, (9) and (10) indicate that the pressure gradient along the y direction is O ( $Gr^{-1/4}$ ), which implies that the lowest order pressure gradient along x direction can be determined from the inviscid flow solution. However, this pressure is zero since there is no externally induced free stream. Thus, the elimination of ( $\partial p^*/\partial y^*$ ) between (9) and (10) leads to the following equation:

$$u^* \frac{\partial u^*}{\partial x^*} + v^* \frac{\partial u^*}{\partial y^*} = (1 + \sigma_x^2) \frac{\partial^2 u^*}{\partial y^{*2}} + \frac{\theta}{1 + \sigma_x^2} [\sin(\varphi) + \sigma_x \cos(\varphi)] - \frac{u^{*2} \sigma_x \sigma_{xx}}{1 + \sigma_x^2} \quad (12)$$

In order to remove the singularity at the leading edge Yao [8], we use the following transformation:

$$X=x^*; \quad Y=\frac{y^*}{(4x^*)^{1/4}}; \quad U=\frac{u^*}{(4x^*)^{1/2}}; \quad V=(4x^*)^{1/4}v^* \quad (13)$$

Substituting (13) into (8), (11) and (12), we obtain

$$(4X) \frac{\partial U}{\partial X} + 2U - Y \frac{\partial U}{\partial Y} + \frac{\partial V}{\partial Y} = 0 \quad (14)$$

$$(4X)U \frac{\partial U}{\partial X} + (V - YU) \frac{\partial U}{\partial Y} + 2U^2 = (1 + \sigma_x^2) \frac{\partial^2 U}{\partial Y^2} + \frac{\theta}{1 + \sigma_x^2} [\sin(\varphi) + \sigma_x \cos(\varphi)] - \frac{4XU^2 \sigma_x \sigma_{xx}}{1 + \sigma_x^2} \quad (15)$$

$$(4X)U \frac{\partial \theta}{\partial X} + (V - YU) \frac{\partial \theta}{\partial Y} = \frac{1}{Pr} \left[ (1 + \sigma_x^2) + \frac{4}{3Rd} (\theta + \beta)^3 \right] \frac{\partial^2 \theta}{\partial Y^2} \quad (16)$$

The term Rd on the right-hand side of (16) represents the radiation parameter defined by:

$$Rd = \frac{k \sigma_R}{4 \sigma_B \Delta T^3}$$

According to Ali et al. [14], Rd depends to the nature of the fluid, some values of Rd for different fluid are: (1) Rd = 10–30: carbon dioxide (100–650°F) with corresponding Prandtl number range 0.76–0.6; (2) Rd = 30–200: ammonia vapor (120–400°F) with corresponding Prandtl number range 0.88–0.84; (3) Rd = 30–200: water vapor (220–900°F) with corresponding Prandtl number 1.

The corresponding boundary conditions in the (X, Y) coordinates are:

$$Y = 0; U = V = 0; \theta = 1 \\ Y \rightarrow \infty: U = 0; \theta = 0 \quad (17)$$

One of the most important parameters in heat transfer analysis is the local Nusselt number defined as:

$$Nu = - \frac{Lq_w}{k(T_w - T_\infty)} \quad (18)$$

where k is thermal conductivity and  $q_w$  is the heat flux at the wall given by:

$$q_w = k \vec{n} \cdot \nabla T$$

here

$$\vec{n} = \left\{ -\frac{\sigma_x}{\sqrt{1 + \sigma_x^2}}, \frac{1}{\sqrt{1 + \sigma_x^2}} \right\} \quad (20)$$

where  $\vec{n}$  is the unit vector normal to the wavy surface. Using boundary layer variables (6) and (13), we obtain

$$Nu_x = -(1 + \sigma_x^2)^{1/2} \left( \frac{Gr}{4X} \right)^{1/4} \left( \frac{\partial \theta}{\partial Y} \right)_{Y=0} \quad (21)$$

### III. NUMERICAL METHOD

In the present study, a marching finite differences scheme was used to discretize the coupled equations (14)–(16) for U, V and  $\theta$ . The algebraic systems of equations were solved using Gauss-Seidel algorithm with a relaxation coefficient equal to 0.7 for the variables U and V and to 0.5 for  $\theta$ . The convergence criterion for U, V and  $\theta$  is based on the relative errors between two iterations supposed to be inferior to  $10^{-5}$ . Moreover, grid independency checks were made. Some of the calculations were tested using various space meshes. We have come to the conclusion that to choose of 100×90 was adequate to the modeling of the natural convection along the inclined wavy plate.

We have also compared in Table I our numerical results for the local Nusselt number at different X locations of the wavy surface, for  $Rd \rightarrow \infty$ ,  $Pr=1$  and  $A=0.1$  with those of Kumari et al [15] as well as by Chiu and Chou [16]. Through this comparison, it was found that the present numerical method is suitable for this study. The small difference in some points may be attributed to the different methods used.

TABLE I  
COMPARISON OF  $Nu/(Gr/4X)^{1/4}$ ,  $A=0.1$ ,  $Rd \rightarrow \infty$ ,  $Pr=1$

X	Kumari et al. [15]	Chiu and Chou [16]	Present
1.5	0.53634	0.53591	0.53474
1.75	0.5481	0.56203	0.51
2	0.53709	0.53479	0.53178
2.25	0.54732	0.56241	0.50842
2.5	0.53762	0.53362	0.5324
2.75	0.54674	0.56362	0.56554
3	0.53804	0.53245	0.53481

No vertical lines in table. Statements that serve as captions for the entire table do not need footnote letters.

<sup>a</sup>Gaussian units are the same as cgs emu for magnetostatics; Mx = maxwell, G = gauss, Oe = oersted; Wb = weber, V = volt, s = second, T = tesla, m = meter, A = ampere, J = joule, kg = kilogram, H = henry.

#### IV. RESULTS AND DISCUSSION

The controlling parameters of the fluid flow and heat transfer rates for this problem are, Prandtl number ( $Pr=1$ ), the dimensionless amplitude wavelength ratio ( $A=0-0.3$ ), the inclination angle  $\phi$  of the wavy plate from the horizontal in the range ( $20^\circ-90^\circ$ ) and the radiation parameter  $Rd$  ( $50-200$ ).

##### A. Effects of the Amplitude Wavelength

The velocity profiles at a given  $X$  ( $X=0.5$ ), for  $Pr=1$ ,  $Rd=200$  and  $\phi=60^\circ$  are presented in Fig. 2 (a), this figure shows that the magnitude of velocities decrease as the amplitude of the waves increases, while the hydrodynamic boundary layer thickness increases. Fig. 2 (b) represents the velocity contours for the wavy plate ( $A=0.2$ ), it is seen from this figure that the crests of the wavy surface are at  $X=0.5, 1, 1.5, 2$  etc. while the troughs are at  $X=0.25, 0.75, 1.25$  etc. It is obvious that the hydrodynamic boundary layers are thicker near the crests of the wavy surface than the troughs. It is also observed from this figure that the velocity contours occur a periodical phenomenon except, when  $Y$  is in the range ( $0.5-1.5$ ) the shape of the sinusoidal is changed, it is clearly seen recirculation zones in this range and this is because the velocity increases in the  $Y$  range ( $0-0.5$ ) and then decreases when ( $Y > 1.5$ ) as seen in Fig. 2 (a).

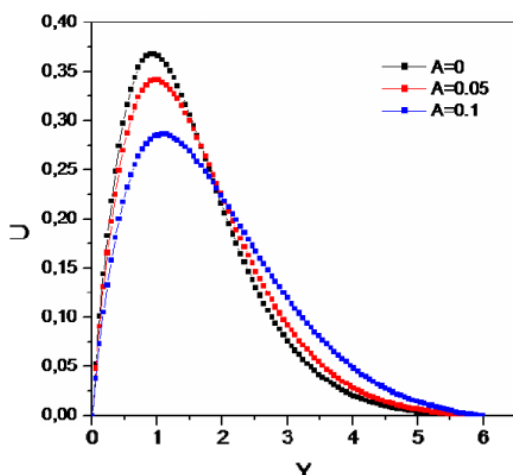


Fig. 2 (a) Velocity profiles for different amplitude wavelength

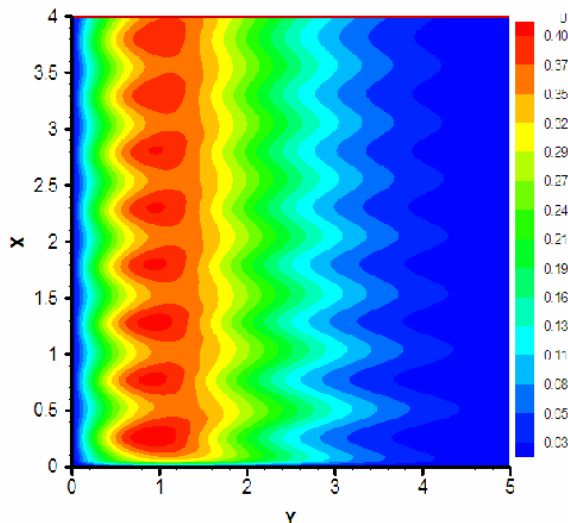


Fig. 2 (b) Velocity contours:  $A=0.1$

The temperature profiles at a given  $X$  ( $X=0.5$ ), the local Nusselt number for  $Pr=1$ ,  $Rd=200$ ,  $\phi=60^\circ$  and for different values of the amplitude wavelength are presented in Figs. 3, 4. It is observed from Fig. 3 that higher amplitude wavelength leads to increase the thermal boundary layer thickness, while the local Nusselt number  $Nu$  takes behavior of the wavy surface and the maximum values occur on the crests of the wavy surface while the minimum values occur on the troughs as shown in Fig. 4. Additionally, the isotherms are presented in Fig. 5 which clearly illustrates a sinusoidal behavior and the isotherms lines spread along the wavy plate; the highest temperatures are restricted in the troughs because heat is transferred in these zones to fluid essentially by conduction.

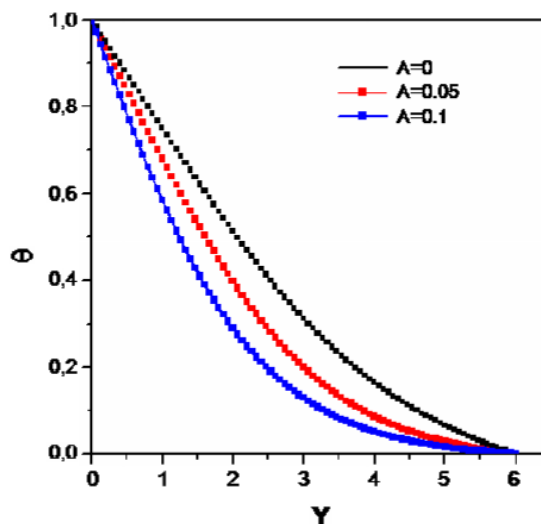


Fig. 3 Temperature profiles for different values of the amplitude wavelength

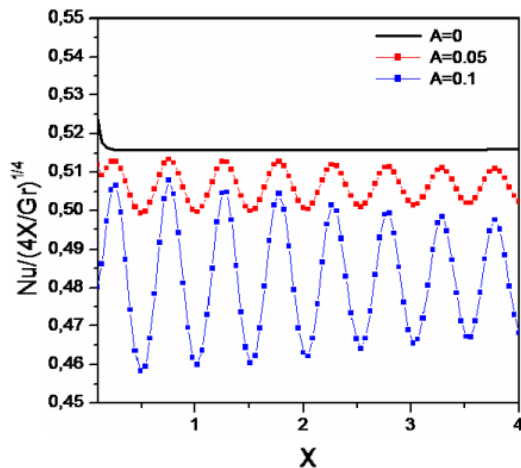


Fig. 4 Effects of the amplitude wavelength on the local Nusselt number

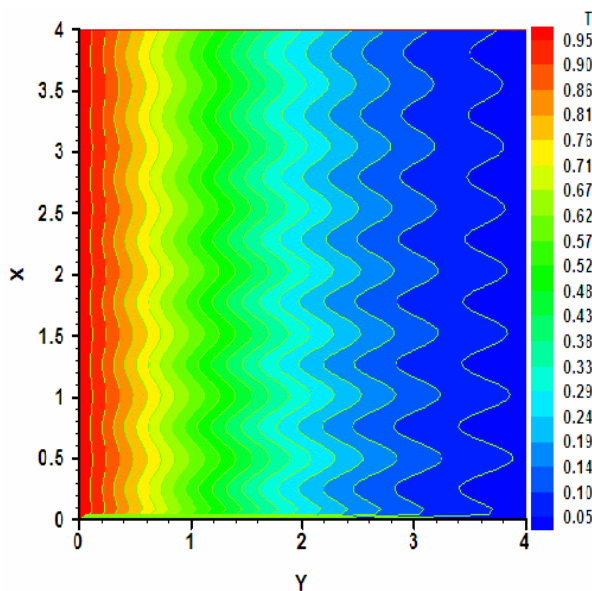


Fig. 5 Velocity contours:  $A=0.1$

#### B. Effects of the Inclination Angle

The effect of the inclination angle from the horizontal of the wavy plate on the velocity, temperature and local Nusselt number for  $A=0.1$  and  $Rd=200$  is presented in Figs. 6, 7. It is seen from Fig. 5 that increasing of the inclination angle ( $20^\circ$ – $90^\circ$ ) leads to increase the maximum of the dimensionless velocity and the heat transfer rate as shown in Fig. 6, while the thermal boundary layer thickness decreases as observed in Fig. 7. This is can be explained that increasing of the angle inclination increases the effect of the buoyancy force due to thermal diffusion by a factor of  $\sin(\varphi)$ . Consequently, the driving force to the fluid increases as a result velocity of the fluid increases. Moreover, when the thermal boundary layer decreases the transfer by convection is important than the transfer by conduction and this is leads to increase the heat transfer rate.

It is worth noting that our study is not valuable for a small inclination angle, this is because the boundary layer approximation for (2) is not valuable in this case.

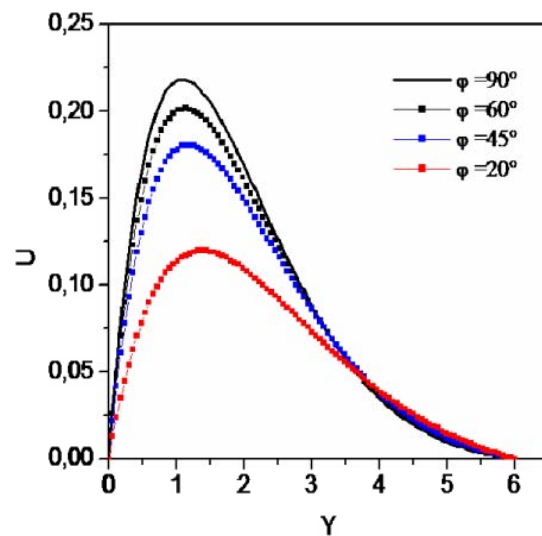


Fig. 6 Effects of the inclination angle on the velocity profiles

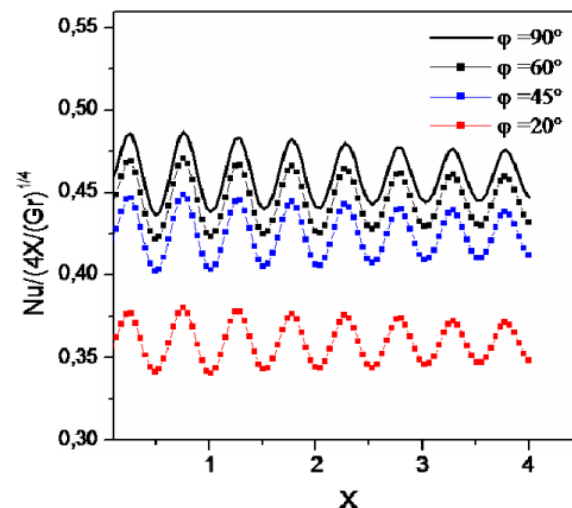


Fig. 7 Effects of the inclination angle on the local Nusselt number

#### C. Effects of the Radiation Parameter

For an inclination angle ( $\varphi = 60^\circ$ ) and  $A=0.1$ , the effects of radiation parameter  $Rd$  (50–200) on velocity profiles, temperature profiles and heat transfer rate are plotted in Figs. 8–10. It is observed from Fig. 8 that increasing of  $Rd$  leads to decrease the velocity profiles and the hydrodynamic boundary layer as well as the temperature profiles and the thermal boundary layer as shown in Fig. 9. Consequently, increasing of the radiation parameter  $Rd$  increases the local Nusselt as observed in Fig. 10.

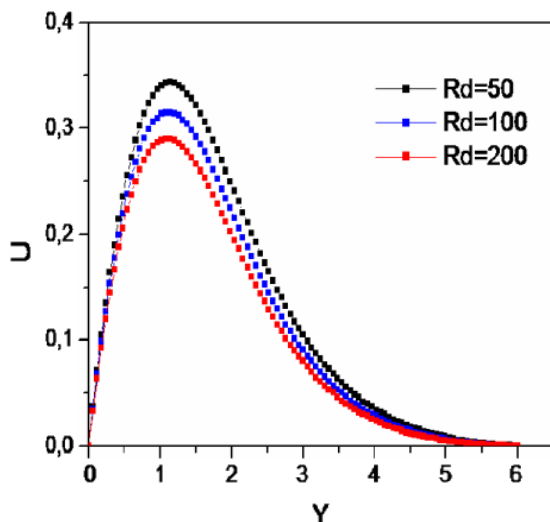


Fig. 8 Effects of the radiation parameter on the velocity profiles

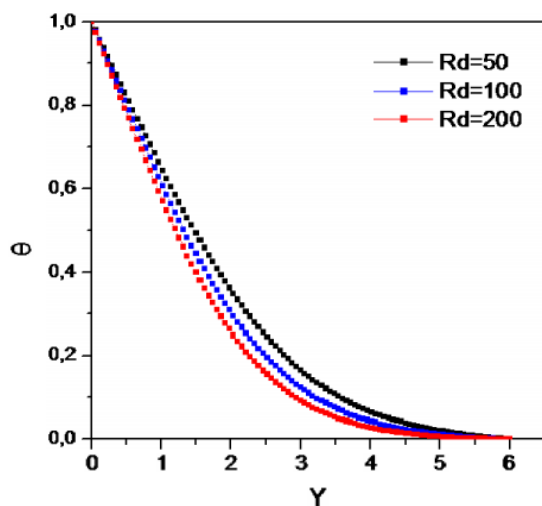


Fig. 9 Effects of the radiation parameter on the temperature profiles

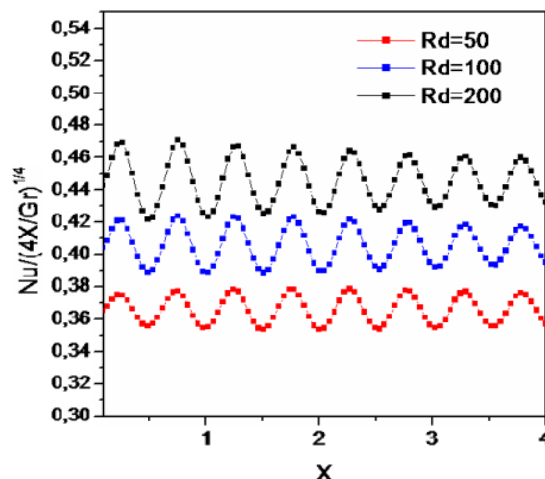


Fig. 10 Effects of the radiation parameter Rd on the local Nusselt number

## V. CONCLUSION

The effects of thermal radiation on free convection in the boundary layer along an inclined wavy surface have been studied numerically. The boundary-layer equations were discretized with a finite differences scheme and solved using Gauss-Seidel iterative method. The effects of amplitude wavelength ratio, the inclination angle and the radiation parameter on momentum and heat transfer have been studied in detail.

From this present work, it has been found that the wavy surface disturbs the flow whatever the effects of the parameters Rd and  $\phi$ . The higher amplitude wavelength ratio decreases the velocity profiles while heat transfer rate is higher in the crests. Increasing of inclination angle from the horizontal of the wavy plate leads to increase the maximum of the dimensionless velocity and the heat transfer rate. It is also found that increasing of the radiation parameter Rd leads to decrease the velocity profiles and the temperature profiles while the local Nusselt number increases.

## REFERENCES

- [1] J.A. Adams, MC. Fadden and P.W. Aiche, " Simultaneous Heat and Mass Transfer in Free Convection with Opposing Body Forces," *J. Numer. Heat Transfer*, vol. 12, pp. 642-647,1966.
- [2] L.S. Yao, " Natural convection along a wavy surface," *ASME, J. Heat Transfer*, vol. 105 , pp. 465-468, 1983.
- [3] C. Ching-Yang, "Natural convection heat and mass transfer near a vertical wavy surface with constant wall temperature and concentration in a porous medium," *Int. Comm. Heat and Mass Transfer*, Vol. 27, n° 8, pp. 1143-1154, 2000.
- [4] S. Kefeng, S. and L. Wen-Qiang, "Time evolution of double-diffusive convection in a vertical cylinder with radial temperature and axial solute gradients," *Int. J. Heat mass transfer*, vol. 49, pp. 995-1003, 2006.
- [5] J. Jer-Huan, Wei-Mon and L. Yan Hui-Chung, "Natural convection heat and mass transfer along a vertical wavy surface," *Int. J. of Heat and Mass Transfer*, vol. 46, pp. 1075-1083, 2003.
- [6] H.T Lin, W.S. Yu and S.L. Yang, "Free convection on an arbitrarily inclined plate with uniform surface heat flux," *Wärme-Stoffübertrag.*, vol. 24, pp. 183-190, 1989.
- [7] S. Shyam, T.K , Rajeev, K.G. Rohit , and K. Aiyub , "MHD Free convection radiation interaction along a vertical surface embedded in

- darcean porous medium in presence of sores and dufour's effects," *J. Thermal Science*, vol. 14, n° 1, pp. 137-145, 2010.
- [8] S. Whitaker, "Radiant Energy Transport in Porous Media," *Int. Engng. Chem. Fund.*, vol. 19, n° 2, pp. 210-218, 1980.
- [9] B.C. Chandrasekhara., P. Nagaraju, "Composite heat transfer in the case of a steady laminar flow of a gray fluid with small optical density past a horizontal plate embedded in a saturated porous media", *Wärme-Stoffübertrag.*, vol. 23, n° 6, pp. 343-352, 1988.
- [10] A. Raptis, "Radiation and Free Convection Flow through a Porous Medium," *Int. Comm Heat Mass Transfer*, vol. 25, n° 2, pp. 289-295, 1998.
- [11] M. A. Hossain, I. Pop, "Radiation Effect on Darcy Free Convection Flow along on Inclined Surface placed in Porous Media," *J. Heat and Mass Transfer*, vol. 32, n° 4, pp. 223-227, 1997.
- [12] A. J., Chamkha, "Solar radiation assisted convection in uniform porous medium supported by a vertical flat plate," *Trans. ASME. J. Heat Transfer*, vol. 119, pp. 89-96, 1997.
- [13] EM. Sparrow, RD. Cess, "Free convection with blowing or suction," *J. Heat Trans-T ASME* vol. 83, pp. 387-396, 1961.
- [14] MM. Ali, TS. Chen, BF. Armaly., "Natural convection-radiation interaction in boundary-layer flow over horizontal surfaces," *AIAA J.*, vol. 22, pp.1797-1803, 1984.
- [15] M. Kumari, I. Pop, H.S. Thakha., "Free convection boundary layer flow of non newtonian fluid along a vertical wavy surface," *Int. J. Heat and fluid flow*, vol. 18 n° 6, pp. 625-631, 1997.
- [16] Chiu, C.P. and Chow, H.M., "Free convection in the boundary layer flow of micropolar fluid along a vertical wavy surface," *Acta Mechanica*, vol. 101, pp. 161-174, 1993.